Bonding Analysis of Inorganic Transition-Metal Cubic Clusters. 6. Copper(I)−Dithiolato Species and Related Compounds

Maria Teresa Garland,[†] Jean-François Halet,[‡] and Jean-Yves Saillard*[,‡]

Laboratorio de Cristalografía, Universidad de Chile, Casilla 487-3, Santiago, Chile, and Laboratoire de Chimie du Solide et Inorganique Moléculaire, UMR-CNRS 6511, Institut de Chimie de Rennes, Université de Rennes 1, 35042 Rennes Cedex, France

Received April 18, 2000

Extended Hückel and density functional calculations carried out on 128-MVE Cu_8(dithiolato)$_6$ edge-bridged cubic clusters indicate that their stability is mainly driven by the chelating effect of the ligands, which provide a stable 16-electron configuration to the approximately trigonal planar metal centers. Nevertheless, a weak but significant $d^{10}-d^{10}$ bonding interaction is present which is rather independent from the dithiolato bite effect. The metal centers have a nonbonding $4p_z$ vacant AO pointing to the center of the cube available for bonding to an encapsulated atom. The electronic closed-shell requirement is satisfied for the 136-MVE and 140-MVE counts, respectively, when a main-group atom or a transition-metal atom is incorporated in the middle of the cube. The bonding within these dithiolato compounds is compared to other edge-bridged M_8 cubic clusters. In particular, it is shown that clusters of higher nuclearity but containing an M_8 cubic core are related to the dithiolato species. Indeed, their outer metal atoms can be considered as belonging to the ligand shell, interacting with the M_8 cube in a way similar to the dithiolato ligands in the Cu_8 species.

1. Introduction

Although cubic transition-metal clusters are far less common than octahedral clusters, they are nowadays well documented in the literature.[1] Investigations of the electronic structure of some of them by us[2] and by others[3] have contributed to a rationalization of their bonding and an understanding of their stability and properties. From this perspective, it is interesting to note that the first type of octanuclear cubic transition-metal complexes which was ever characterized, namely, the Cu^I dithiolato species,[4] has not yet been subjected to any theoretical study, apart for an early semiempirical investigation of a Cu_8S_{12} model by Avdeef and Fackler.[5] This prompted us to undertake a combined extended Hückel (EH)/density functional (DF) study of the whole family of these copper clusters as well as of some related compounds.

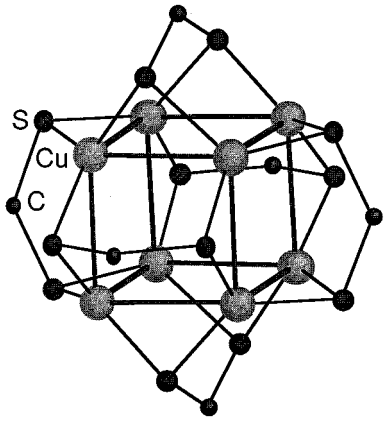

$[Cu_8(i\text{-MNT})_6]^{4-}$
1

The various dithiolato ligands used to stabilize these Cu^I cubic frameworks are depicted in Chart 1. In 1968 Fackler and coworkers characterized the first member of this series, namely, $[Cu_8(i\text{-MNT})_6]^{4-}$ (**1**), as a phenyltrimethylammonium salt.[4a] Since then, other compounds containing the same cluster core architecture have been published.[4] They are reported in Table 1, together with their major structural characteristics. In all of them, except $[Cu_8(MNT)_6]^{4-}$ (see below), each sulfur atom of the bidendate ligands bridges an edge of the Cu_8 cube in such a way that the 12 sulfur atoms describe a distorted icosahedron. The S···S vector of each individual dithiolato ligand lies perpendicular to one of the faces of the cube. Consequently, the whole cluster architecture exhibits the idealized T_h symmetry (see **1**). Each metal center is bonded to 3 sulfur atoms in a 3-fold

[†] Universidad de Chile.
[‡] Université de Rennes 1.

(1) For example, see the following and references therein: (a) Halet, J.-F.; Saillard, J.-Y. *Struct. Bonding* **1997**, *87*, 81. (b) Gautier, R.; Halet, J.-F.; Saillard, J.-Y. In *Metal Clusters in Chemistry;* Braunstein, P., Oro, L., Raithby, P. R., Eds.; Wiley-VCH: New York, 1999; Vol. 3, p 1643.
(2) (a) Furet, E.; Le Beuze, A.; Halet, J.-F.; Saillard, J.-Y. *J. Am. Chem. Soc.* **1994**, *116*, 274. (b) Furet, E.; Le Beuze, A.; Halet, J.-F.; Saillard, J.-Y. *J. Am. Chem. Soc.* **1995**, *117*, 4936. (c) Zouchoune, B.; Ogliaro, F.; Halet, J.-F.; Saillard, J.-Y.; Eveland, J. R.; Whitmire, K. H. *Inorg. Chem.* **1998**, *37*, 865. (d) Gautier, R.; Halet, J.-F.; Saillard, J.-Y. *Eur. J. Inorg. Chem.* **1999**, 673. (e) Gautier, R.; Ogliaro, F.; Halet, J.-F.; Saillard, J.-Y.; Baerends, E. J. *Eur. J. Inorg. Chem.* **1999**, 1161.
(3) (a) Burdett, J. K.; Miller, G. J. *J. Am. Chem. Soc.* **1987**, *109*, 4081. (b) Hoffman, G. G.; Bashkin, J. K.; Karplus, M. *J. Am. Chem. Soc.* **1990**, *112*, 8705. (c) Rösch, N.; Ackermann, L.; Pacchioni, G. *Inorg. Chem.* **1993**, *32*, 2963.
(4) (a) McCandish, L. E.; Bissel, E. C.; Coucouvanis, D.; Fackler, J. P., Jr.; Knox, K. *J. Am. Chem. Soc.* **1968**, *90*, 7357. (b) Dietrich, H. *Acta Crystallogr.* **1978**, *A32*, S26. (c) Dietrich, H.; Storck, W.; Manecke, G. *Makromol. Chem.* **1981**, *182*, 2371. (d) Hanhui, Z.; Xiufen, Y. *Jiegou Huaxue (J. Struct. Chem.)* **1989**, *8*, 132. (e) Hollander, F. J.; Coucouvanis, D. *J. Am. Chem. Soc.* **1974**, *96*, 5647. (f) Hollander, F. J.; Coucouvanis, D. *J. Am. Chem. Soc.* **1977**, *99*, 6268.
(5) Avdeef, A.; Fackler, J. P., Jr. *Inorg. Chem.* **1978**, *17*, 2182.

10.1021/ic0101937 CCC: $20.00
Published on Web 05/26/2001

Table 1. Selected Structural Data of Clusters Containing a $(Cu^I)_8$ Cubic Framework

compound	MVE count	Cu···Cu (Å) dist: av (range)	av S−Cu−S angle (deg)	S···S bite dist of the ligand (Å)	av Cu−S dist (Å)	av Cu−(μ_8-E) dist (Å)	ref
$[Cu_8(i\text{-MNT})_6]^{4-}$ (**1**)[a]	128	2.83 (2.78−2.87)	119	3.08	2.25		4a,e
$[Cu_8(i\text{-MNT})_6]^{4-}$ (**1**)[b]	128	2.84 (2.74−2.88)	119	3.07	2.25		4b,c
$[Cu_8(i\text{-MNT})_6]^{4-}$ (**1**)[c]	128	2.80 (2.76−2.87)	119	3.08	2.25		4d
$[Cu_8(DTS)_6]^{4-}$	128	2.84 (2.78−2.87)	116	3.92	2.25		4e,f
$[Cu_8(DED)_6]^{4-}$	128	2.79 (2.76−2.88)	118	3.04	2.26		4e,f
$[Cu_8(MNT)_6]^{4-}$ (**3**)	128	3.36 (3.09−3.72)	120	3.37	2.22		4b,c
$Cu_8[S_2P(O^iPr)_2]_6(\mu_8\text{-S})$ (**2**)	136	3.09 (3.08−3.10)	119	3.53	2.28	2.69	9a
$Cu_8[S_2P(OEt)_2]_6(\mu_8\text{-S})$	136	3.01 (2.95−3.07)	119	3.45	2.27	2.60	9b
$\{Cu_8[S_2P(OEt)_2]_6(\mu_8\text{-Cl})\}^+$	136	3.23 (3.02−3.44)	118	3.50	2.30	2.57	9c
$\{(Cu^I)_8(Cu^{II})_6[SC(Me)_2CH_2NH_2]_{12}(\mu_8\text{-Cl})\}^{7+}$ (**7**)	136	3.31 (3.26−3.34)	120	3.35	2.28	2.87	23a
$\{(Cu^I)_{8(Cu^{II})_6}[SC(Me)_2COO]_{12}(\mu_8\text{-Cl})\}^{5-}$	136	3.35 (3.33−3.38)	120	3.39	2.28	2.90	23b
$[(Cu^I)_8(Cu^{II})_6(\text{D-Pen})_{12}(\mu_8\text{-Cl})]^{5-}$[d]	136	3.30 (3.24−3.37)	120	3.38	2.27	2.85	23c

[a] Phenyltrimethylammonium salt. [b] Tertrabutylammonium salt. [c] Tetraethylammonium salt. [d] D-Pen = D-penicillaminato.

Chart 1. Some Dithiolato Ligands Used To Stabilize Cu_8 Cubic Architectures and Their Simplified Models Considered in the Calculations

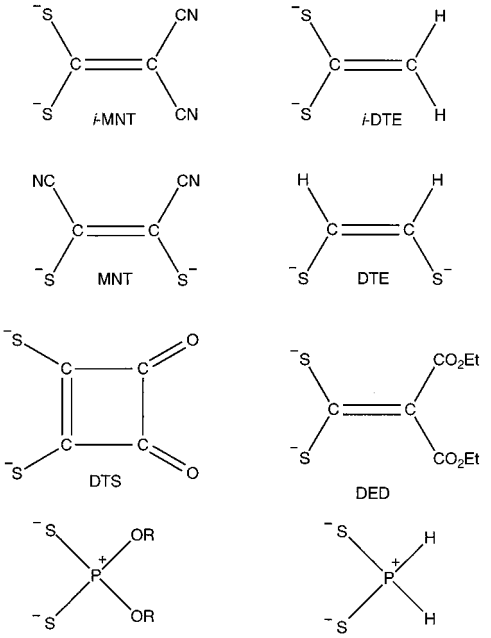

and nearly planar coordination mode (see Table 1). This is a stable geometry for 16-electron d^{10} metal complexes,[6] and one is tempted to describe these 128 metal valence electron (MVE) clusters as made of 8 noninteracting 16-electron trigonal planar copper centers kept together in the same molecule by the chelating effect of the dithiolato ligands.

However, the reported Cu···Cu separations (2.76−2.88 Å, see Table 1) are consistent with the possibility of direct metal−metal bonding. The achievement of the 18-electron configuration in **1** would require a Cu−Cu bond order of 2/3. This would correspond to the existence of 8 occupied Cu−Cu bonding molecular orbitals (MO) and 16 unoccupied antibonding counterparts. Another explanation of the short Cu···Cu contacts would be the existence of so-called $d^{10}-d^{10}$ (or closed-shell−closed-shell) type bonds. A simple orbital explanation of $d^{10}-d^{10}$ bonding in Cu^I complexes was provided by Mehrotra and Hoffmann in the late 1970s.[7] They described it as resulting from the mixing of bonding combinations of high-lying and vacant 4s and 4p atomic orbitals (AO) with occupied and mainly nonbonding 3d combinations. In a recent review on closed-shell interactions, Pyykkö[8] stressed the importance of electron correlation and relativistic effects (at least for the heavier transition metals) in this particular type of bonding. The question of the existence or the absence of Cu···Cu bonding in the title clusters has been debated several times in the literature,[4e,f,5] but no firm answer has been provided on the basis of modern theoretical calculations. This is one of the reasons which pushed us to undertake this study.

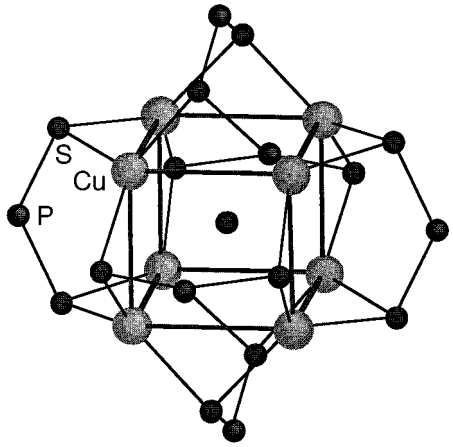

$Cu_8(S_2P(O^iPr)_2)_6(\mu_8\text{-S})$
2

Another reason for our interest in these compounds is that some of them have been shown to incorporate an encapsulated main-group atom (see Table 1),[9] as exemplified by $Cu_8[S_2P(O^iPr)_2]_6(\mu_8\text{-S})$ (**2**), made by Fackler and co-workers.[9a] We were interested in comparing the nature of the bonding between the Cu_8 cage and its host with that of other atom-centered cubic clusters which we have analyzed previously.[1,2b,e] Moreover, we were also interested in investigating theoretically the possibility of incorporating transition-metal atoms, as observed in other examples of cubic clusters.[1]

2. Computational Details

EH calculations[10] were carried out using the CACAO package.[11] The CACAO standard atomic parameters were used. Unless specified in the text, the following bond distances (Å) were assumed in the

(6) Albright, T. A.; Burdett, J. K.; Wangbo, M.-H. *Orbital Interactions in Chemistry*; John Wiley & Sons: New York, 1985.
(7) Mehrotra, P. K.; Hoffmann, R. *Inorg. Chem.* **1978**, *17*, 2187.
(8) Pyykkö, P. *Chem. Rev.* **1997**, *97*, 597.
(9) (a) Liu, C. W.; Stubbs, T.; Staples, R. J.; Fackler, J. P., Jr. *J. Am. Chem. Soc.* **1995**, *117*, 9778. (b) Huang, Z. X.; Lu, S. F.; Huang, J. Q.; Wu, D. M.; Huang, J. L. *Jiegou Huaxue (J. Struct. Chem.)* **1991**, *10*, 213. (c) Wu, D.; Huang, J. Q.; Lin, Y. Huang, J. L. *Sci. Sin. Ser. B. (Engl. Ed.)* **1988**, *31*, 800.

calculated models: Cu···Cu = 2.85; Cu−(μ_2-S) = 2.25; S−C = 1.72; C═C = 1.34; C−H = 1.09; S−P = 1.98; P−H = 1.42. Calculations on experimental X-ray structures were carried out with data obtained from the Cambridge Data Base system.[12] This data base was also used to supply some of the metrical parameters given in Table 1.

DF calculations were carried out using the Amsterdam Density Functional (ADF) package developed by Baerends and co-workers.[13] Unless specified in the text, the results discussed in this paper were obtained assuming the local density approximation (LDA) of electron correlation using the Vosko−Wilk−Nusair parametrization.[14] Most of the models considered were also calculated at the nonlocal density approximation (NLDA) assuming the corrections of Becke[15] and Perdew[16] for the exchange and correlation energies, respectively. LDA and NLDA calculations gave similar results, except for the optimized Cu···Cu separations which were found to be ≈5% too long at the NLDA level, as compared to the experimental values. Spin-unrestricted (ULDA and UNLDA) calculations were performed for all the considered open-shell systems. The standard ADF basis set IV was used for the atoms constituting the Cu_8X_{12} and $Cu_8X_{12}(\mu_8\text{-X})$ (X = S, Cl) cores, which describes the valence 3d(Cu), 4s(Cu), 3s(X), and 3p(X) orbitals with triple-ζ Slater-type orbitals, and the 4p(Cu) and 3d(X) orbitals with a single-ζ polarization function. The standard basis set II, which describes the valence shells with double-ζ functions, was employed for the other atoms. The frozen-core approximation was used to treat the core electrons. Since the ADF program does not work with T_h symmetry, geometry optimizations on the Cu_8 species having this symmetry were carried out assuming D_{2h} symmetry instead, with the additional constraint of all the Cu···Cu separations being equal. Such a procedure allows rapid geometry convergence toward a molecular structure which is very close to T_h symmetry and avoids problems caused by the very soft potential energy surface around its minimum (the Cu_8 cubes were found to be very flexible). We have checked on several models that full geometry optimizations assuming other T_h subgroups lead to very similar energies and optimized structures.

3. 128-MVE Cu^I_8(dithiolato)$_6$ Clusters

(a) Qualitative Approach. With the help of EH calculations carried out on models of the characterized compounds listed in Table 1, it has been possible to build a general qualitative MO picture of the Cu_8^I(dithiolato)$_6$ clusters (see Figure 1a,b). We start with the MO level ordering of a single Cu^I atom lying in the same ligand environment as observed in **1**. It is sketched in Figure 1a where the well-known pattern of a vacant nonbonding $4p_z$-type AO lying far above a block of five low-lying occupied 3d levels emerges.[6] In the cubic cluster the 8 trigonal planar Cu^I centers interact in the way depicted in Figure 1b. The contracted Cu 3d AOs overlap rather weakly to give rise to a set of 40 occupied combinations which are nonbonding, weakly bonding, or weakly antibonding. Overall, the 3d interactions are somewhat destabilizing since all of these combinations are occupied. The more diffuse $4p_z$ AOs overlap significantly. Therefore, their combinations are found over a somewhat larger energy range of about 3 eV. However, their energy remains high and consequently none of them is occupied. The ordering

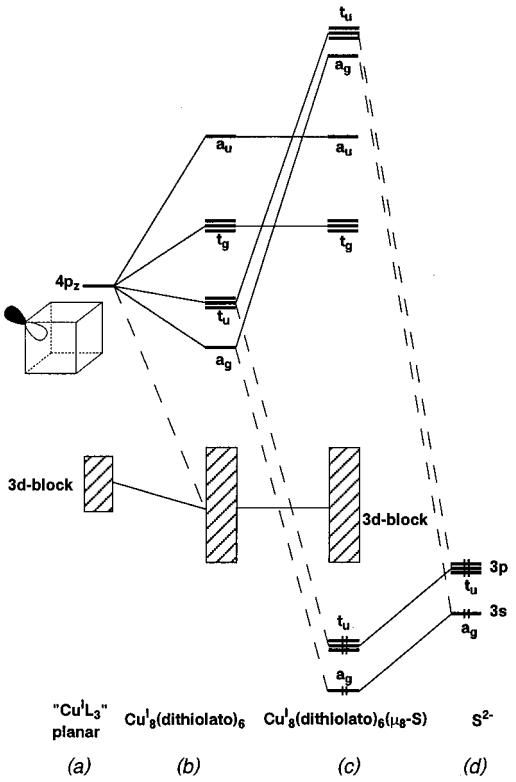

Figure 1. (a) Frontier orbitals of a noninteracting tricoordinated Cu^I center isolated from a 128-MVE Cu^I_8(dithiolato)$_6$ cluster; (b) general MO level ordering for a 128-MVE Cu^I_8(dithiolato)$_6$ cluster resulting from the interaction of eight 16-electron tricoordinated Cu^I centers; (c) general MO level ordering of a 136-MVE Cu^I_8(dithiolato)$_6(\mu_8$-S) cluster resulting from the interaction of the 128-MVE empty cage (b) and an encapsulated S^{2-} atom (d).

of these vacant levels is a_g (bonding) < t_u (bonding) < t_g (antibonding) < a_u (antibonding) in idealized T_h symmetry. At this stage of the analysis it is clear that the existence of Cu···Cu contacts does not correspond to a situation in which some unambiguously bonding levels are occupied and some antibonding counterparts are vacant. None of the $4p_z$ in-phase combinations is occupied nor is any out-of-phase 3d combination vacant. Clearly, the formal Cu−Cu bond order is zero. However, the $4p_z$ combinations can mix with the occupied 3d combinations of the same symmetry, provided that the $\langle Cu(4p_z)|Cu(3d)\rangle$ overlap along the edges is significant enough. The largest mixing is expected to involve the bonding a_g and t_u $4p_z$ combinations (dashed lines in Figure 1a,b), which lie much closer in energy to the 3d levels than their antibonding counterparts. This so-called second-order mixing of empty bonding levels into occupied ones, if any, could be the factor responsible for the short Cu···Cu contacts. This is typically the situation for d^{10}−d^{10} bonding described by Mehrotra and Hoffmann.[7]

A qualitative evaluation of these weak stabilizing interactions can be traced by looking at the Cu···Cu overlap populations computed in the various models (Table 2). The corresponding values are all positive but very small, suggesting very weak bonding. Clearly, the repulsion arising from the interactions between the occupied 3d levels is nearly balanced by the stabilizing $4p_z$−3d mixing. It is important to note that in general EH-computed overlap populations between nonbonded atoms are dominated by 4-electron repulsions and are found to be significantly negative. For example, the overlap populations corresponding to the S···S contacts inside the thiolato ligands of our calculated models lie in the range −0.050 to −0.123. Values close to zero are unusual and are often indicative of

(10) (a) Hoffmann, R. *J. Chem. Phys.* **1963**, *39*, 1397. (b) Ammeter, J. H.; Bürgi, H.-B.; Thibeault, J. C.; Hoffmann, R. *J. Am. Chem. Soc.* **1978**, *100*, 3686.
(11) Mealli, C.; Proserpio, D. *J. Chem. Educ.* **1990**, *67*, 399.
(12) *Cambridge Data Base System*, Cambridge Crystallographic Data Center, Version 5.12.
(13) (a) Baerends, E. J.; Ellis, D. E.; Ros, P. *Chem. Phys.* **1975**, *8*, 41. (b) Baerends, E. J.; Ros, P. *Int. J. Quantum Chem.* **1978**, *S12*, 169. (c) Boerrigter, P. M.; te Velde, G.; Baerends, E. J. *Int. J. Quantum Chem.* **1988**, *33*, 87. (d) te Velde, G.; Baerends, E. J. *J. Comput. Phys.* **1992**, *99*, 84.
(14) Vosko, S. D.; Wilk, L.; Nusair, M. *Can. J. Chem.* **1990**, *58*, 1200.
(15) (a) Becke, A. D. *J. Chem. Phys.* 1**986**, *84*, 4524. (b) Becke, A. D. *Phys. Rev. A.* **1988**, *38*, 3098.
(16) (a) Perdew, J. P. *Phys. Rev. B* **1986**, *33*, 8882. (b) Perdew, J. P. *Phys. Rev. B* **1986**, *34*, 7406.

Table 2. Selected Computed Data on Cluster Models Having a $(Cu^I)_8$ Cubic Framework[a]

compound	MVE count	Cu···Cu EH overlap population	HOMO−LUMO gap (eV) EH	HOMO−LUMO gap (eV) DF	Cu···Cu dist (Å)	X−Cu−X angle (deg)	X···X bite dist (see text) (Å)	Cu−X dist (Å)	Cu−(μ_8-E) dist (Å)	DF Mulliken atomic net charges Cu (cube)	DF Mulliken atomic net charges (μ_8-E)	bonding energy (eV) between $(\mu_8\text{-E})^{-/2-}$ anion and 128-MVE cage[d]
$[Cu_8(i\text{-DTE})_6]^{4-}$ (**1′**)	128	0.005	3.88	2.05	2.86	119	3.11	2.27		0.115		
$[Cu_8(DTE)_6]^{4-}$	128	0.000	2.98	1.55	2.80	116	3.78	2.28		0.119		
$[Cu_8(S_2PH_2)_6]^{2+}$	128	0.004	5.12	2.12	3.17	120	3.69	2.25		0.149		
$Cu_8(S_2PH_2)_6$	130	0.004	0.65	0.85	2.74	115	3.75	2.27		0.125		
$[Cu_8(DTE)_6]^{4-}$ (**3′**) C_i sym[b]	128	0.000	3.62	2.55	3.45	119	3.38	2.27		0.192		
$[Cu_8Cl_{12}]^{4-}$ [c]	128	0.009	4.36	1.09	2.88	113	3.83	2.30		0.216		
$[Cu_8Cl_{12}]^{6-}$ [c]	130	0.009	0.91	2.44	2.51	104	3.95	2.51		0.166		
$[Cu_8(i\text{-DTE})_6(\mu_8\text{-S})]^{6-}$	136	−0.007	3.28	1.51	2.76	117	3.13	2.40	2.40	0.052	−0.022	12.93
$[Cu_8(DTE)_6(\mu_8\text{-S})]^{6-}$	136	−0.010	2.60	1.34	2.84	115	3.80	2.40	2.46	0.067	0.059	13.34
$Cu_8(S_2PH_2)_6(\mu_8\text{-S})$ (**2′**)	136	−0.008	5.88	1.20	2.84	116	3.73	2.33	2.46	0.086	0.060	−20.38
$[Cu_8(S_2PH_2)_6(\mu_8\text{-Cl})]^{+}$	136	−0.010	5.81	2.00	3.12	119	3.71	2.28	2.70	0.119	−0.040	−8.18
$[(Cu^I)_8(Cu^{II})_6(\mu\text{-SMe})_{12}(NH_3)_{12}(\mu_8\text{-Cl})]^{7+}$ (**7′**)[e]	136	−0.007	0.02	0.22	3.13	120	3.18	2.29	2.72	0.201	−0.131	−20.21
$[Cu_8(S_2PH_2)_6(\mu_8\text{-Cu})]^{+}$	140	−0.005	3.74	1.45	2.92	117	3.72	2.28	2.53	0.064	0.367	−7.95
$[Cu_8(S_2PH_2)_6(\mu_8\text{-Cu})]^{3+}$	138	−0.005	1.40	1.01	3.01	119	3.65	2.25	2.60	0.054	0.540	−0.47

[a] The optimized metrical data were obtained from DF-LDA calculations (X = heteroatom of the surrounding ligands, i.e., S or Cl). Unless specified, all the considered molecular structures are of T_h symmetry (see text). [b] Assuming the same molecular arrangement as compound **3** (see text). [c] O_h symmetry. [d] A positive value indicates repulsive interaction. [e] $S = 3$ ground state.

very soft attractive potentials.[7] In order to check that no other effect is present, calculations were also carried out with the 3d AOs removed from the basis set. The result is that the Cu···Cu overlap populations get even closer to zero but with a negative sign, indicating the absence of any other orbital effect.

(b) DFT Calculations. The major data computed at the LDA level (see Computational Details) are given in Table 2. The optimized geometries obtained with the *i*-DTE and DTE model ligands are in good agreement with the corresponding experimental values reported for the related clusters containing *i*-MNT, DTS, and DED ligands.[4a−f] They do not correlate with the so-called bite effect of the dithiolato ligands which would tend to induce longer Cu···Cu separations in the case of DTE which has a larger S···S bite distance (see Table 2). This insensitivity of the Cu···Cu separation to the bidendate bite effect was recognized a long time ago by Hollander and Coucouvanis, who compared several cluster molecular structures.[4e,f] It was interpreted as a clue for the existence of some Cu···Cu bonding which forces the metal−metal separation to be roughly constant over the series of considered ligands, regardless of the different bite effects of the different ligands. However, the optimized Cu···Cu distance is longer in the case of the $(S_2PH_2)^-$ ligand, but still not correlated with the bidendate bite effect (Table 2). Clearly, the chemical nature of the ligands plays a significant role in the strength of the weak Cu···Cu interaction. Only clusters bearing chemically related dithiolato ligands exhibit similar Cu···Cu distances, irrespective of the bite effect.

At this stage of the discussion, it is interesting to note that the cluster $[Cu_8(MNT)_6]^{4-}$ (**3**) adopts a ligand arrangement which is different from that of the other characterized 128-MVE dithiolato species.[4b,c] The MNT units, which incidentally also have a rather large bite distance (Table 1), are bridging the Cu_8 cube in a less symmetrical fashion than in **2**. Six of the Cu atoms are connected to two S atoms of the same MNT unit and to one S atom of another ligand. The two other Cu atoms are connected to three S atoms belonging to two different MNTs. In principle, this arrangement, which also provides the metal with a trigonal planar coordination mode, could adopt the ideal D_{3d} symmetry. In fact, the X-ray structure of cluster **3** exhibits a wide range of Cu···Cu distances[4b,c] (see Table 1), lowering its symmetry to C_i. This is consistent with the larger average Cu···Cu distance, which suggests no significant bonding. Calculations have been made on the cluster model $[Cu_8(DTE)_6]^{4-}$ (**3′**) under the C_i symmetry constraint (Table 2). It was found to be 1.47 and 1.91 eV more stable than its T_h isomer at the LDA and NLDA levels, respectively. The LDA-optimized Cu···Cu distances were found to lie within the 3.30−3.84 Å range, suggesting no significant interaction. This ligand arrangement allows a smaller bite distance for the DTE ligand than in the T_h isomer (3.38 vs 3.78 Å), which may be more favorable with respect to ligand stability. It also provides a local environment of the 16-electron metals which is more planar than in the T_h isomer (Table 2).

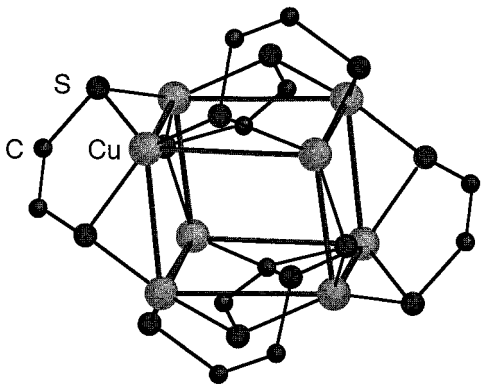

$[Cu_8(MNT)_6]^{4-}$

3

In order to cancel completely the chelating bite effect, the dithiolato ligands were replaced by individual isolobal main-group atomic anions. To maintain a reasonable charge on the whole cluster, chloride ions were preferred to sulfide ions. The results obtained with the 128-MVE $[Cu^I_8(\mu\text{-}Cl)_{12}]^{4-}$ model are given in Table 2. The general features of its electronic structure are similar to those of the other calculated models. The Cu···Cu separation (2.88 Å) is only slightly larger than those found for the dithiolato species. Geometry optimizations assuming various symmetry constraints indicate that the chlorine ligand shell prefers to describe a cuboctahedron rather than a distorted

icosahedron, giving rise to O_h symmetry for the whole cluster. Clearly, the T_h symmetry of the Cu_8S_{12} core observed for the title dithiolato clusters is imposed by the chelating effect of the ligands.

(c) Related Species. The 128-MVE Cu^I_8(dithiolato)$_6$ title compounds are related to the hypothetical $[Cu^I_8(\mu\text{-}Te_2)_6]^{4-}$ cluster which was theoretically investigated[17a,18] as a model for the building block of several solid-state copper polytelluride compounds characterized by Kanatzidis and co-workers.[17] In all of these phases, the 128-MVE $Cu_8(Te_2)_6$ cage contains an encapsulated alkaline or alkaline-earth cation which is supposed to be ionically bonded to the cage. Indeed, the $[Cu^I_8(\mu\text{-}Te_2)_6]^{4-}$ cage is isoelectronic and isostructural with the 128-MVE dithiolato species, with the $(Te-Te)^{2-}$ anions occupying the same position with respect to the Cu_8 cube as the S···S vectors of the dithiolato ligands. As a matter of fact, the Cu···Cu separations in Kanatzidis's compounds are of the same order of magnitude as those reported in Table 1.[17] The formal reduction of each Te_2^{2-} ligand by 2 electrons is expected to break the Te−Te single bonds and provide a structure like that of the $[Cu^I_8(\mu\text{-}Cl)_{12}]^{4-}$ model.

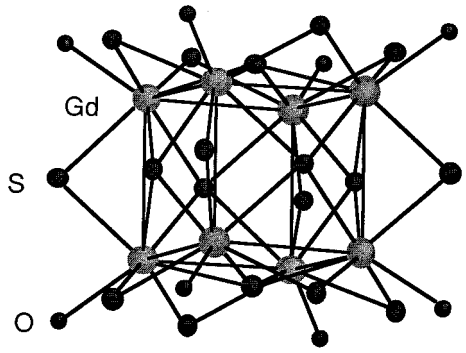

$Gd_8(\mu_4\text{-}S_6)(\mu\text{-}SPh)_{12}(thf)_8$

4

A series of 100-MVE clusters of the type $Ln_8(\mu_4\text{-}E)_6(\mu\text{-}E'Ph)_{12}(thf)_8$ (E, E′ = S, Se) (**4**) has been recently characterized by Brennan and co-workers.[19] In addition to the 12 edge-bridging ER groups, there are six face-bridging chalcogen atoms. **4** consists of the assemblage of 7 heptacoordinated metal centers. No formal bond is expected between these d^0 metal centers, nor a closed-shell−closed-shell attraction as in the Cu^I species. However, the reported metal−metal separations (average = 3.82 Å in the case of Ln = Gd[19a]) could be consistent with some weak bonding. This is confirmed by EH calculations on the experimental structure of the Gd cluster which found a significantly positive Gd···Gd overlap population (+0.026). This attractive interaction results from the mixing of Gd···Gd bonding combinations of vacant metal orbitals into occupied ligand levels (through-bond interaction).

(17) (a) Zhang, Y.; Park, Y.; Hogan, T.; Schindler, J. L.; Kannewurf, C. R.; Seong, S.; Albright, T. A.; Kanatzidis, M. G. *J. Am. Chem. Soc.* **1995**, *117*, 10300. (b) Park, Y.; De Groot, D. C.; Schindler, J. L.; Kannewurf, C. R.; Kanatzidis, M. G. *Angew. Chem., Int. Ed. Engl.* **1991**, *30*, 1325. (c) Park, Y.; Kanatzidis, M. *Chem. Mater.* **1991**, *3*, 781.

(18) Poblet, J.-M.; Rohmer, M.-M.; Bénard, M. *Inorg. Chem.* **1996**, *35*, 4073.

(19) (a) Melman, J. H.; Emge, T. J.; Brennan, J. G. *Chem. Commun.* **1997**, 2269. (b) Freedmann, D.; Emge, T. J.; Brennan, J. G. *J. Am. Chem. Soc.* **1997**, *119*, 1112.

4. Main-Group-Centered Cu^I_8(dithiolato)$_6$(μ_8-E) (E = S, Cl) 136-MVE Clusters

(a) Qualitative Approach. A qualitative description of the bonding between the encapsulated S^{2-} anion and the $\{Cu_8[S_2P(O^iPr)_2]_6\}^{2+}$ host in **2** was provided by Fackler and co-workers.[9a] The corresponding orbital interaction scheme, illustrated in Figure 1b−d, was fully reproduced by EH calculations on the $\{Cu_8[S_2PH_2]_6\}^{2+}$ model. The occupied 3s (a_g) and 3p (t_u) AOs of the encapsulated S^{2-} atom interact in a stabilizing way with the unoccupied a_g and t_u 4p_z combinations of the 128-MVE Cu^I_8(dithiolato)$_6$ cage. Therefore, the bonding of the encapsulated atom is delocalized over 8 Cu−S contacts. On average, the cage consists of eight 17-electron centers (i.e., can be described by two mesomeric forms, each having four 16-electron and four 18-electron centers). The computed (μ_8-S)−Cu overlap populations in our various models are about 2.5 times smaller than the corresponding (μ_2-S)−Cu values (0.184 vs 0.443 in $Cu_8(S_2PH_2)_6(\mu_8\text{-}S)$, for example). The occupation of the μ_8-S AOs in $Cu_8(S_2PH_2)_6(\mu_8\text{-}S)$ after interaction is 1.65 and 1.70 in each of the 3p and the 3s orbitals, respectively. These values indicate significant covalent interaction between the copper cage and the inserted sulfur atom.

Interestingly, once the S^{2-} atom is incorporated in the 128-MVE cage, the Cu···Cu overlap population is computed to be slightly negative (see Table 2). At first sight this is counter-intuitive since the participation of the 4p_z a_g and t_u bonding combinations into occupied (μ_8-S)−Cu in-phase levels (Figure 1b−d) is expected to induce additional stabilizing Cu···Cu interaction. Indeed, after interaction with S^{2-}, the (4p_z) a_g orbital of the $[Cu_8(S_2PH_2)_6]^{2+}$ cage is occupied by 0.48 electron, whereas each component of the t_u 4p_z level is occupied by 0.42 electron. The reason for this computed trend originates from the fact that some occupied 3d in-phase combinations of the cage also interact with S^{2-} and, therefore, mix somewhat into the vacant a_g and t_u levels. The resulting depopulation of these in-phase 3d levels weakens the Cu···Cu bonds. This destabilization slightly dominates the interaction at the EH level. Again, these calculations suggest that the weak Cu···Cu interactions in these clusters result from a delicate balance between 3d and 4p_z effects.

(b) DFT Calculations. DFT calculations performed on the considered model complexes confirm the qualitative picture of Figure 1c. The major results are given in Table 2. The optimized geometries of $Cu_8(S_2PH_2)_6(\mu_8\text{-}S)$ (**2′**) and $[Cu_8(S_2PH_2)_6(\mu_8\text{-}Cl)]^+$ can be compared to the experimental structures of $Cu_8(S_2P(OR)_2)_6(\mu_8\text{-}S)$ (R = ^{i}Pr (**2**) and Et)[9] and $[Cu_8(S_2P(OEt)_2)_6(\mu_8\text{-}Cl)]^+$.[9c] The agreement is satisfactory, except for the optimized Cu···Cu distances which are about 0.2 Å shorter than the experimental ones (see Tables 1 and 2). For all but one of the calculated dithiolato models, a shortening of the Cu···Cu separation is observed upon incorporation of S^{2-} or Cl^- anion inside the cage. Conversely, an elongation of the Cu−X distance is observed. This trend was also reproduced at the NLDA level. It can be attributed to the ionic component of the bonding between the encapsulated anion and the cationic cage. The positively charged Cu atoms are attracted by the central anion, causing a contraction of the Cu_8 cube. On the other hand, the negatively charged X outer ligand atoms are repelled from the center of the cube. It is possible that these ionic interactions are overestimated by the DF calculations since the optimized cube edges are shorter than the experimental ones.

An estimation of the bonding between the 128-MVE cage and its encapsulated anion can be provided by DF calculations. The corresponding LDA bonding energies in the model clusters

are given in Table 2. They were calculated as the difference between the energy of the optimized filled cluster and the sum of the energies of S^{2-} (or Cl^-) and of the optimized 128-MVE empty cluster. Some of these bond dissociation energies were also calculated at the NLDA level, yielding values of the same order of magnitude (for example, −18.91 vs −20.32 eV and −7.17 vs −6.18 eV in the cases of $Cu_8(S_2PH_2)_6(\mu_8\text{-}S)$ (**2′**) and $[Cu_8(S_2PH_2)_6(\mu_8\text{-}Cl)]^+$, respectively). All the bond energies associated with negatively charged empty cages are positive, indicating in turn repulsive interactions. Obviously, even if it is overestimated within the DF calculations, the ionic component of the bond dissociation energy is important. A really bonding interaction is only found for the two models of the experimentally characterized $Cu_8[S_2P(OR)_2]_6(\mu_8\text{-}S)$ and $\{Cu_8(S_2P(OEt)_2)_6(\mu_8\text{-}Cl)\}^+$ compounds for which the empty cage is positively charged. The question of the covalent vs ionic nature of this bond in **2** has been addressed by Fackler and co-workers.[9a] Whereas EH calculations are unable to account for ionic interactions, the ADF program can provide a decomposition of the bonding energy between unrelaxed fragments according to a procedure described by Ziegler,[20] which considers an electrostatic term as well as Pauli repulsion and orbital interaction terms. In the case of **2′**, the bonding energy between the unrelaxed fragments is −21.16 eV. Its electrostatic, Pauli repulsion, and orbital interaction components are −48.45, 37.73, and −10.44 eV, respectively. As expected, the orbital interaction term is made of two major components: a_g (−3.08 eV) and t_u (−6.98 eV). Clearly, the ionic component of the bond between the encapsulated S^{2-} anion and its 128-MVE cage is dominating. A similar conclusion can be drawn for the $[Cu_8(S_2PH_2)_6(\mu_8\text{-}Cl)]^+$ model, in which the electrostatic, Pauli repulsion, and orbital interaction terms are −15.37, 10.31, and −3.25 eV, respectively. The importance of the electrostatic component of the bond dissociation energy is not reflected in the computed atomic net charges (Table 2) which indicate significant electron transfer from S^{2-} (or Cl^-) to its 128-MVE cage. This can be understood in realizing that this electrostatic term is computed from the densities of the unperturbed fragments, i.e., the densities of the isolated, noninteracting fragments. Once the bond is allowed to establish, charge transfer occurs.

Examples of edge-bridged distorted M_8 cubic frameworks centered with a main-group atom are reported.[21,22] The tetrahedral distortions of their metal frameworks allow the encapsulated atoms to be rather sp^3-hybridized and bonded to only 4 metal atoms. Although these compounds differ in many ways from the title clusters (see below), we have checked our models to see if such a tetrahedral distortion is possible. Calculations did not yield geometries significantly different from ideal T_h symmetry.

(c) Related Octanuclear Species. A series of 144-MVE octanuclear centered clusters of general formula $[M(ER)_{16}(E')]^{n-}$ in which E and E′ are main-group atoms and M is Cd or Zn have been characterized by Dance and co-workers.[21] As exemplified by $[Cd_8(SePh)_4(\mu\text{-}SePh)_{12}(\mu_4\text{-}S)]^{2-}$ (**5**),[21c] the metal cube is tetrahedrally distorted such that the sulfur atom is bonded to only 4 Cd atoms. The 4 remaining Cd atoms hold a supplementary SePh terminal ligand so that all the metals are tetrahedrally coordinated and satisfy the 18-electron rule. From the total MVE count (144 = 8 × 18), no metal−metal bond is expected. d^{10}−d^{10} bonding is also unlikely with Cd^{II}. As a matter of fact, the molecular structures of these compounds do not indicate any attractive interaction (the shortest Cd···Cd contact in **5** is 4.078 Å). This is supported by EH calculations carried out on the experimental structure of **5** which found weakly repulsive Cd···Cd overlap populations (≈−0.02).

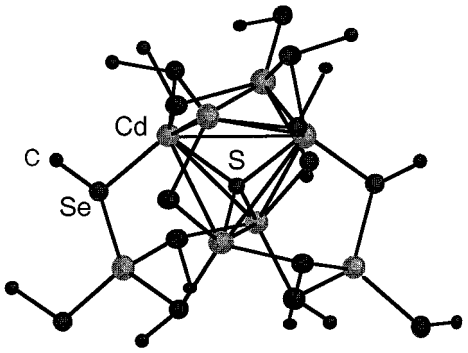

$[Cd_8(SePh)_4(\mu\text{–}SePh)_{12}(\mu_4\text{-}S)]^{2-}$

5

The compound $[Cu_4Mn_4(\mu\text{-}S^iPr)_{12}(\mu_4\text{-}S)]^{2-}$ (**6**) exhibits a similar (but weaker) tetrahedral distortion of the cube as in **5**, with the central S atom bonded to the Mn centers only.[22] As a result, the open-shell Mn^{II} atoms are tetrahedrally coordinated while the 16-electron Cu centers have approximate trigonal planar environments. No formal metal−metal bond is expected in this situation. The experimental Mn···Cu contacts (average = 3.092 Å) could be consistent with some very weak bonding, as supported by the corresponding EH average overlap populations (+0.001). The nonbonding Cu···(μ_4-S) EH overlap populations indicate some attraction (+0.034).

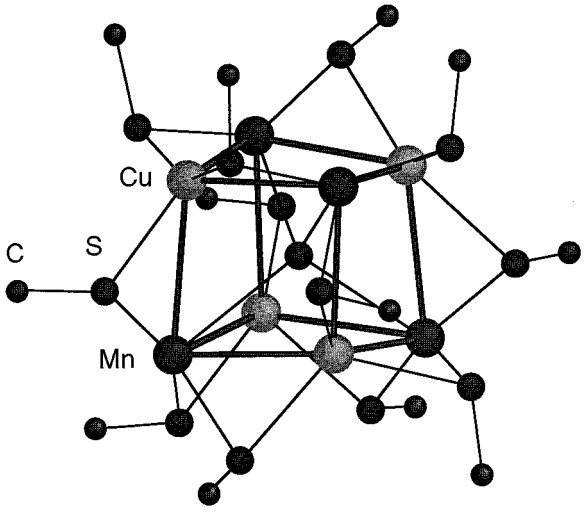

$[Cu_4Mn_4(\mu\text{–}S^iPr)_6(\mu_4\text{-}S)]^{4-}$

6

(d) Related Species of Higher Nuclearity. There are mixed-valent Cu_{14} clusters,[23] such as $\{Cu^I_8Cu^{II}_6[SC(Me_2)CH_2NH_2](\mu_8\text{-}Cl)\}^{7+}$, the core of which is shown in **7**,[23a] which are structurally related to the 136-MVE Cu_8^I(dithiolato)$_6(\mu_8\text{-}E)$ species (see Table 1). They consist of a Cl-centered cube of trigonal planar

(20) Ziegler, T. In *Metal Ligand Interactions: From Atoms to Clusters to Surfaces*; Salahub, D. R., Russo, N., Eds.; Kluwer: Dordrecht, 1992; p 367.

(21) (a) Dance, I. G. *J. Chem. Soc., Chem. Commun.* **1980**, 818. (b) Dance, I. G. *Aust. J. Chem.* **1985**, *38*, 1391. (c) Lee, S. A.; Fisher, K. J.; Craig, D. C.; Scudder, M. L.; Dance, I. G. *J. Am. Chem. Soc.* **1990**, *112*, 6435.

(22) Stephan, H.-O.; Kanatzidis, M. G.; Henkel, G. *Angew. Chem., Int. Ed. Engl.* **1996**, *35*, 2135.

Table 3. Experimental M···M Distances in **8** and **9** and Selected Computed Data on Models of **8**, $\mathbf{8}^{6-}$, and **9**[a]

compound	MVE count	distance (Å) (EH-OP)			
		$M_{int}\cdots M_{int}$	$M_{int}\cdots M_{ext}$	$M_{ext}\cdots M_{ext}$	$M_{int}\cdots(\mu_8\text{-E})$
$Cu_{20}(PEt_3)_{12}(\mu_5\text{-Se})_{12}(\mu_8\text{-Se})$ (**8**)[b]	298	3.01	2.68	2.82	2.61
$Cu_{20}(PH_3)_{12}(\mu_5\text{-Se})_{12}(\mu_8\text{-Se})$ (**8′**)[c]	298	2.96 (+0.001)	2.64 (+0.032)	2.66 (+0.015)	2.56 (+0.192)
$[Cu_{20}(PH_3)_{12}(\mu_5\text{-Se})_{12}(\mu_8\text{-Se})]^{6-}$ ($[\mathbf{8'}]^{6-}$)	304	2.89 (+0.000)	2.58 (+0.029)	2.61 (+0.012)	2.51 (+0.181)
$Pd_{20}(PPh_3)_{12}(\mu_5\text{-As})_{12}$ (**9**)[d]	260	2.81	2.78	3.52	
$Pd_{20}(PH_3)_{12}(\mu_5\text{-As})_{12}$ (**9′**)[b]	260	2.87 (+0.048)	2.79 (+0.050)	3.09 (−0.002)	

[a] Extended Hückel overlap populations (EH-OP) have been calculated assuming experimental averaged geometries of **8** and **9**. The given optimized distances were obtained at the DF-LDA level. The calculated molecular structures are of T_h symmetry. [b] Average experimental values (from ref 25). [c] Calculations assuming $S = 0$. [d] Average experimental values (from ref 26).

Cu^I atoms. The 12 edge-bridging thiolato ligands bear amine or carboxylate functions which bind to 6 external Cu^{II} atoms. The Cu^{II} atoms are in a square planar coordination mode and project to the center of the cube faces, describing thus an octahedron. Assuming that the Cu^{II} atoms are part of the ligand system, these clusters can be considered as 136-MVE Cl-centered Cu_8 cubic clusters. The Cu^I and Cu^{II} atoms lie far apart. The experimental $Cu^I\cdots Cu^I$ distances are of the same order of magnitude as those of the Cu_8^I(dithiolato)$_6(\mu_8$-E) clusters. EH and DF calculations performed on the model $\{Cu^I{}_8[(NH_3)_2Cu^{II}\text{-}(\mu\text{-SMe})_2]_6(\mu_8\text{-Cl})\}^{7+}$ (**7′**) confirm the electronic relationship between the cubic cores of **3** and **7** (Table 2). The ground state of this model was found to have six unpaired electrons, at both the DF-LDA and ULDA levels. This is consistent with the picture of six weakly interacting Cu^{II} centers and in full agreement with the reported magnetic properties of **7**.[23a]

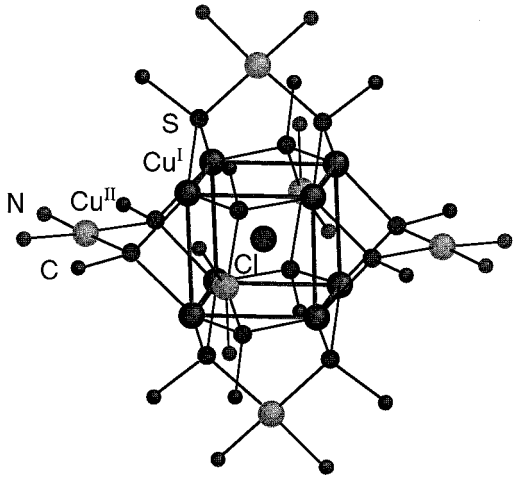

$[Cu_8^ICu_6^{II}(SCMe_2CH_2NH_2)_6(\mu_8\text{-Cl})]^{7+}$

7

The $Cu_{20}Se_{13}(PEt_3)$ cluster (**8**), synthesized by Fenske and Krautscheid,[24] also contains a Cu_8 cube, which is this time centered by an Se atom. As with the centered and noncentered Cu_8 species, the edges of the cube are capped by 12 μ-Se atoms which describe an icosahedron. The 12 external Cu (Cu_{ext}) atoms lie close to the Se_{12} shell. They also bridge the edges of the cube, and they bear a phosphine ligand. The overall idealized symmetry is T_h. Some experimental geometrical parameters of **8** are given in Table 3. There is strong similarity between the $Cu_8(\mu\text{-E})_{12}(\mu_8\text{-E})$ cores of **2** (Table 1) and **8** (Table 3). In addition to the bonds within this core, **8** exhibits short $Cu_{ext}\cdots Cu_{ext}$ and $Cu_{ext}\cdots Cu_{int}$ contacts (Cu_{int} = atom from the inner Cu_8 cube). The Cu_{ext} atoms are also bonded to 3 Se atoms. The 12 external Se atoms are attached to 3 Cu_{ext} and 2 Cu_{int} centers. This hypercoordination mode led us to consider that all the electrons of the Se atoms are involved in cluster bonding. This leads to the 322-MVE count for **8**. Assuming that the 12 external Se atoms retain a nonbonding lone pair would give 298 MVEs.[24] Since there is no Se···Se contact, the chalcogen oxidation state is −II. This leads to a noninteger average metal oxidation state ($Cu^{+1.3}$).

EH calculations on the model (**8′**) in which the PEt_3 ligands were replaced by PH_3 found a small HOMO−LUMO gap (0.27 eV), suggesting the possibility of an open-shell configuration. DF geometry optimizations of **8′** at the LDA and NLDA levels and assuming a closed-shell configuration led to similar gaps (0.18 and 0.26 eV, respectively). Several low-lying configurations and spin states are expected because the LUMO and the HOMO are of t_u and t_g symmetries, respectively. The singlet state was found to be the ground state at the ULDA level, while UNLDA calculations found the triplet state $(t_g)^5(t_u)^1$ to be the ground state, lying 0.10 eV below the singlet state. Unfortunately, there are no magnetic measurements reported so far on **8** to be compared with these DFT results. The geometries of the different low-lying states are almost identical, exhibiting less than 1% variation on the optimized bond distances, in agreement with the nonbonding character of the t_u and t_g orbitals.

As said above, the closed-shell configuration of **8** is associated with a small HOMO−LUMO gap. On the other hand, it exhibits a large gap above the low-lying t_g LUMO: 5.34, 1.84, and 1.53 eV at the EH, LDA, and NLDA levels, respectively. This indicates that the most favored closed-shell MVE count for such an architecture is 322 + 6 = 328. For this electron count, all the Cu atoms would be at the +I (d^{10}) oxidation state. This situation would correspond to full occupation of all the levels having a large metal 3d character. Filling of the t_u LUMO of **8**, which is mainly Cu_{int} and Cu_{ext} 3d in character, hardly changes the EH overlap populations (Table 3). In the case of the 328-MVE count which fulfills the closed-shell requirement, it is possible to provide a 2-electron/2-center bonding picture of the cluster, although considerable delocalization is present. As for the other systems analyzed above, this localized approach does not consider any metal−metal bonding. Starting with the Se^{-II} and Cu^I oxidation states and assuming that each of the 12 edge-bridging selenides donates 4 electrons to the centered cube present in $\mathbf{8}^{6-}$, this cube becomes isoelectronic with **2** with a "local" count of 136 MVEs. Four electrons remain available on each hypervalent selenide atom to make three bonds with Cu_{ext} metals (assuming that no lone pair is retained on Se). In a purely localized picture, one bond is a dative bond and two bonds are simple covalent bonds. Being also connected to 3

(23) (a) Schugar, H. J.; Ou, C.-C.; Thich, J. A.; Potenza, J. A.; Felthouse, T. R.; Haddad, M. S.; Hendrickson, D. N.; Furey, W., Jr.; Lalancette, R. A. *Inorg. Chem.* **1980**, *19*, 543. (b) Birker, P. J. M. W. L. *Inorg. Chem.* **1979**, *18*, 3502. (c) Birker, P. J. M. W. L.; Freeman, H. C. *J. Am. Chem. Soc.* **1977**, *99*, 6890.

(24) Fenske, D.; Krautscheid, H. *Angew. Chem., Int. Ed. Engl.* **1990**, *29*, 1452.

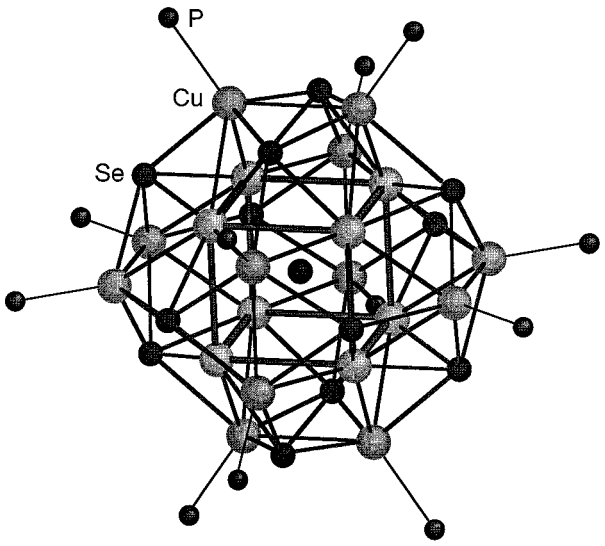

$Cu_{20}(\mu_5\text{-}Se)_{12}(PEt_3)_{12}(\mu_8\text{-}Se)$

8

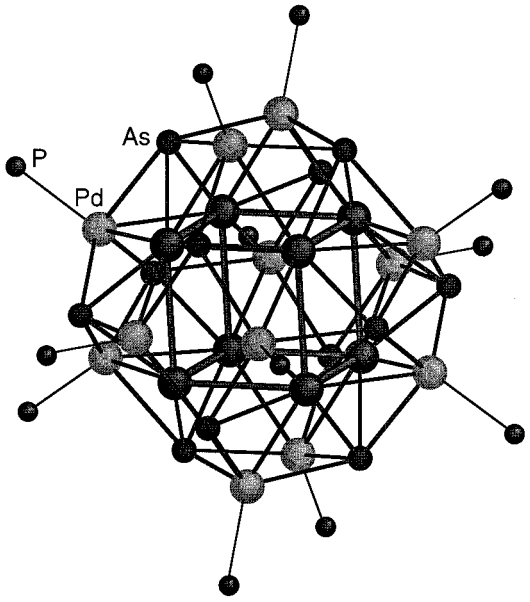

$Pd_{20}(\mu_5\text{-}As)_{12}(PPh_3)_{12}$

9

selenides by one dative and two simple covalent bonds, each d^{10} Cu_{ext} atom receives 4 electrons from the Se ligand shell. Adding the electron pair provided by the attached phosphine, one ends up with a 16-electron configuration for each Cu_{ext} metal center. This is an acceptable electron count for an approximately trigonal planar pyramidal coordination mode.

The Cu···Cu interactions cannot be considered in the above localized picture and have to be added as the result of delocalized $d^{10}-d^{10}$ bonding. Some of the corresponding EH overlap populations (Table 3) are larger than those calculated for the dithiolato species (Table 2). This is partly due to the more favored overlap between the vacant sp hybrid on the capped trigonal planar Cu_{ext} metals[6] and the 3d AOs of their neighbors. These Cu···Cu interactions help to diminish the unsaturation on Cu_{ext}. It should be noted that there is a continuum between $d^{10}-d^{10}$ bonding and the situation where there is a "real" bond. When the mixing of the vacant bonding s/p levels into the occupied levels becomes large, it can be considered as resulting from a level crossing, i.e., the occupied bonding level having dominant s/p character.

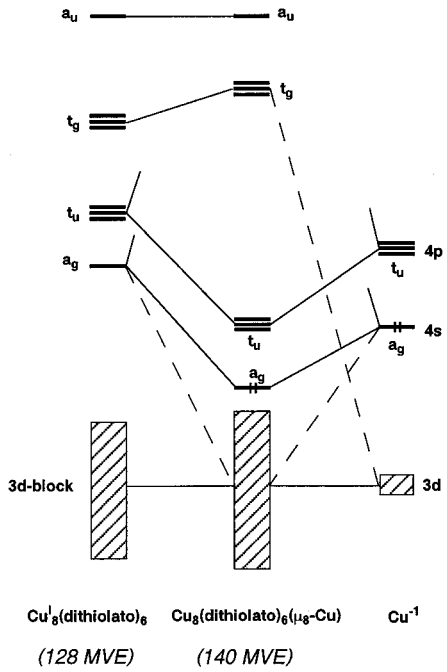

Figure 2. MO interaction diagram for a 140-MVE Cu_8(dithiolato)$_6$-(μ_8-Cu) cluster.

Despite a low-lying LUMO which is essentially nonbonding, the electron-deficient neutral species **8** is stable. The absence of any significant Jahn−Teller distortion away from T_h symmetry is likely to be due to its very high connectivity. This situation is reminiscent of solid-state chemistry and of other highly connected clusters.[1] This electron deficiency is even larger in the related 284-MVE species $Pd_{20}As_{12}(PPh_3)_{12}$ (**9**),[25] in which the metal oxidation state is +1.8. This compound exhibits the same architecture as **8** (see also Table 3), except that there is no atom encapsulated in the central cube. EH and single-point DFT calculations carried out on the $Pd_{20}As_{12}(PH_3)_{12}$ model (**9′**) found no significant HOMO−LUMO gap for any MVE count corresponding to a reasonable cluster charge. In the case of **9**, the top of the 4d band is somewhat Pd−Pd antibonding. Its depopulation tends to strengthen metal−metal bonding, as shown by the experimental $M_{int}\cdots M_{int}$ and $M_{int}\cdots M_{ext}$ separations and the corresponding overlap populations (Table 3).

5. Hypothetical Metal-Centered Cu_8^I(dithiolato)$_6$(μ_8-M) Clusters

Examples of transition-metal cubic clusters encapsulating an additional metal atom are well-documented.[1] Since the reported experimental Cu···Cu distances of the title compounds lie in the range 2.6−3.1 Å (Tables 1 and 3), it is possible to speculate about a centered cubic arrangement in which both types of Cu···Cu separations would lie in this range. The incorporation of a Cu^I atom in a 128-MVE Cu^I_8(dithiolato)$_6$ cluster allows only one bonding interaction involving the occupied t_g set of the 3d AOs of the central metal atom and the vacant $4p_z$ combinations of t_g symmetry of the cage, as sketched in Figure 2. EH calculations on the model $[Cu_8(S_2PH_2)_6(\mu_8\text{-}Cu)]^{3+}$ (with $Cu\cdots Cu_{edge} = 3.20$ Å) indicate that this bonding interaction is weak, as exemplified by the rather small Cu−(μ_8-Cu) overlap

(25) Fenske, D.; Fleischer, H.; Persau, C. *Angew. Chem., Int. Ed. Engl.* **1989**, *28*, 1665.

population (+0.056). This is confirmed by the small negative DF-computed bonding energy (Table 2). Interestingly, the LUMO of $[Cu_8(S_2PH_2)_6(\mu_8\text{-}Cu)]^{3+}$ is a bonding combination of the vacant 4s AO of the central Cu with the $4p_z$ a_1 combination of the Cu_8 cube. This LUMO is low-lying and isolated in the energy scale (Figure 2). Its population strengthens significantly the bond between the cage and its host, as exemplified by the DF bonding energy computed for $[Cu_8(S_2PH_2)_6(\mu_8\text{-}Cu)]^{+}$, which is of the same order of magnitude as that found for $[Cu_8(S_2PH_2)_6(\mu_8\text{-}Cl)]^{+}$ (see Table 2). The decomposition of the bonding energy between the unrelaxed $[Cu_8(S_2PH_2)_6]^{+}$and Cu^{1-} fragments gives −29.95, 24.32, and −5.11 eV for its electrostatic, Pauli repulsion, and orbital interaction components. As expected, the orbital interaction term is made of two major components: a_g (−3.78 eV) and t_g (−0.90 eV) with some significant t_u contribution (−0.55 eV) due to some second-order mixing of the unoccupied t_u bonding contribution into the d-block. A significant charge transfer occurs between the fragments, as reflected by the larger positive charge of the encapsulated Cu atom (Table 2), which by no means can be described as a real Cu^{-I} atom. These results strongly suggest that 140-MVE species of the type $M_8(dithiolato)_6(\mu_8\text{-}M')$ should be stable.

6. Conclusion

The stability of the cubic architecture of the 128-MVE $Cu_8(dithiolato)_6$ clusters is mainly driven by the chelating effect of the ligands. Nevertheless, a weak but significant $d^{10}-d^{10}$ bonding interaction is present which, to some extent, is rather independent of the dithiolato bite effect. To a first approximation, these clusters can be described as made up of 8 almost independent trigonal planar 16-electron metal centers. These metal centers have a nonbonding $4p_z$ vacant AO pointing to the center of the cube. From the diagram of Figure 1b, it seems possible to occupy the a_g $4p_z$ combination which is Cu···Cu bonding. Calculations on the 130-MVE models $Cu_8(S_2PH_2)_6$ and $[Cu_8Cl_{12}]^{6-}$ (Table 2) support this statement.

Incorporation of a main-group atom into the 128-MVE cubic architecture is possible, due to the formation of bonding interactions between the 4 AOs of the main-group atom and appropriate Cu $4p_z$ combinations. This requires the main-group AOs to be fully occupied, leading to the favored 136-MVE count. Calculations also suggest that incorporation of a metal atom should lead to stable species with a favored closed-shell MVE count of 140. In that case the s and three of the d valence AOs of the central atom are involved in the bonding.

Clusters of higher nuclearity but containing a cubic core such as **7**, **8**, and **9** are closely related to the octanuclear species such as **1** and **2**. In these compounds, the outer metal atoms can be considered as belonging to the ligand shell, interacting with the M_8 cube similarly to the 6 dithiolato ligands in **1** and **2**. The high atom connectivity present in **8** and **9** allows them to be both electron-deficient and Jahn−Teller stable. Their electron deficiency allows some metal−metal bonding which provides them with additional stability and some bulk-metal-like properties.

Acknowledgment. Computing facilities were provided by the IDRIS-CNRS computing center of Orsay (France). The CNRS (J.-Y.S.) and CONICYT (M.T.G.) are acknowledged for a cooperative CNRS/CONICYT grant. We are grateful to Prof. M. I. Bruce for helpful comments. Drawings of molecules were prepared with the Ca.R.Ine Cristallographic 3.0.1 program (C. Boudias and D. Monceau, 1989−1994).

IC0101937